ELSEVIER

Cement & Concrete Composites 23 (2001) 255–259

Cement & Concrete Composites

www.elsevier.com/locate/cemconcomp

Surface state analysis by means of confocal microscopy

Jean-Marie Becker, Stéphane Grousson, Michel Jourlin *

Laboratoire Image, Signal et Acoustique, Ecole Supérieure de Chimie Physique, Electronique de Lyon, BP 2077,43 Boulevard du 11 novembre 1918, 69616, Villeurbanne Cedex, France

Abstract

This article aims at the illustration of the potentialities offered by new imaging technologies: in the present case, confocal microscopy. Such an approach gives access to surface information like porosity, wear, cracking and roughness, and is thus a very powerful tool for the evaluation on the surface state of various materials: concrete, ceramics, aluminum alloys, textiles. A perspective is given to exploit and visualize this new data in the best way. © 2001 Elsevier Science Ltd. All rights reserved.

Résumé

Cet article illustre les potentialités offertes par de nouveaux capteurs d'images : dans le cas présent, le microscope confocal. Une telle approche donne accès à des informations surfaciques telles que la porosité, l'usure, la fissuration, la rugosité et apparaît donc comme un outil très puissant pour l'évaluation de l'état de surface de divers matériaux : béton, céramique, alliage d'aluminium, textile. Une perspective est proposée pour exploiter et visualiser ces nouvelles données de la manière la plus efficace. © 2001 Elsevier Science Ltd. All rights reserved.

Keywords: Concrete; Materials; Confocal microscopy; Image processing

1. Introduction: recalls on confocal microscopy

The invention of confocal microscopy in 1957 by Minsky has opened the way for a constant evolution of this technique, due to the progresses in computer science, electronics and optics. Today, there exists two systems based on confocal microscopy: the laser scanning confocal microscopy and that based on a rotating disk [1]. During our study, we used this last kind of system. The tandem scanning microscope (TSM) created by Petran [2] is an improvement of the Minsky system. It consists in a Nipkow disk (Fig. 1) drilled with hundreds of holes (50 μm diameter).

The screening of the sample is realized by the disk rotation. At any time, several holes are lightened by a white light source in order that the sample surface receives incident beams.

The reflected rays will pass back through the disk only if their meeting point with the material is exactly situated in the focus plane (Fig. 2).

In such conditions, at each position of the stage, the sensor (CCD camera) observes the level line situated in the focusing plane, i.e., the intersection of this plane with the sample surface (Fig. 3).

The relief of the sample is then acquired by moving the programmable stage step-by-step along the z-axis (with the adequate resolution). In fact, each point (x, y) of the sample will be seen with a maximum intensity when it lies in the focusing plane.

The knowledge of the stage position gives the z-position of (x, y). We are thus able to attach a gray level at each value of the altitude (for example, brighter pixels correspond to higher altitude). The observed surface is then associated with a topographic image (Fig. 4).

Another information is accessible at the same time: the reflectance of each pixel. In fact, when (x, y) comes in the focus plane during the vertical translation of the stage, its reflectance is maximum but is not the same from a pixel to another. Thus, one defines the reflectance map as the image where each pixel is equipped with its maximal reflectance computed as its maximal observed gray level (Fig. 5).

* Corresponding author.

PII: S0958-9465(00)00081-0

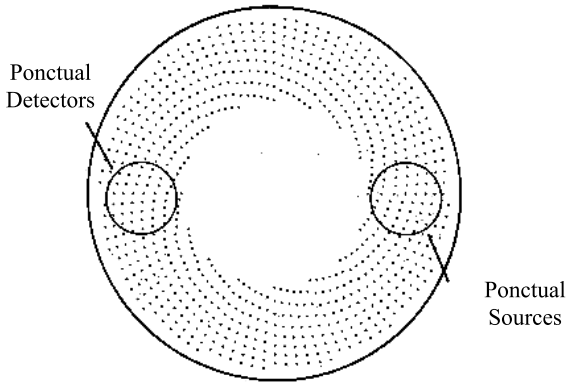

Fig. 1. The Nipkow disk.

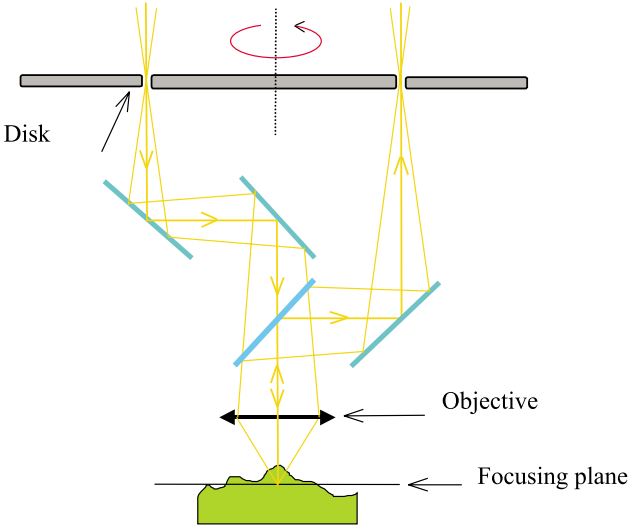

Fig. 2. Optical rays path modelization.

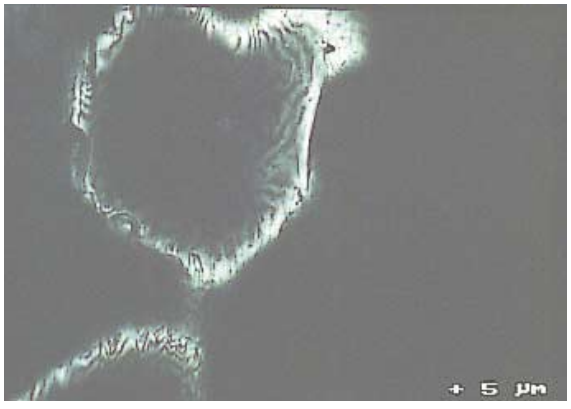

Fig. 3. Visualization of a level line.

Remark 1. In itself, the reflectance image corresponds to an ideally deblurred optical image, independently of the depth: in fact, it is the aggregation of the image slices lying in the successive focusing planes.

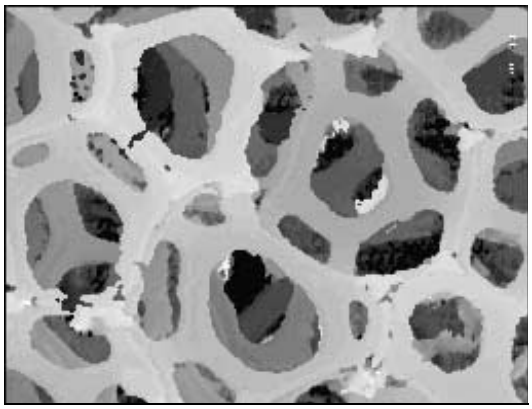

Fig. 4. Topographic image of an electrolytic filter.

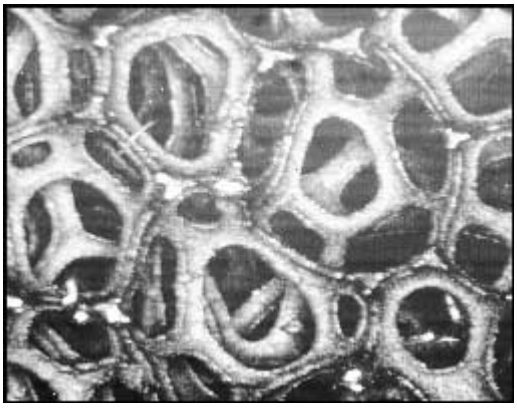

Fig. 5. Reflectance image.

Remark 2. Combined with the topographic image (each point (x, y) is elevated at the altitude corresponding to its gray level in the topographic image), a gray level relief is obtained, conveying a realistic and informative visualization that overwhelms an optical one (Fig. 6).

2. An example: bubbles in a concrete sample

This is a very classical problem: estimating the volume and positioning of air bubbles in a concrete sample. Such an evaluation may be a solution to estimate the sample resistance to frost.

The classical approach consists in an acquisition of the concrete surface submitted to a tangential illumination.

In this case, the porosities corresponding to the bubbles appear as dark objects compared to the "background" (i.e., the concrete surface). Such a method is easy to perform but it does not give a precise estimation of the three-dimensional size and position of the bubbles: the unique information directly accessible is the size of the intersections between the concrete surface

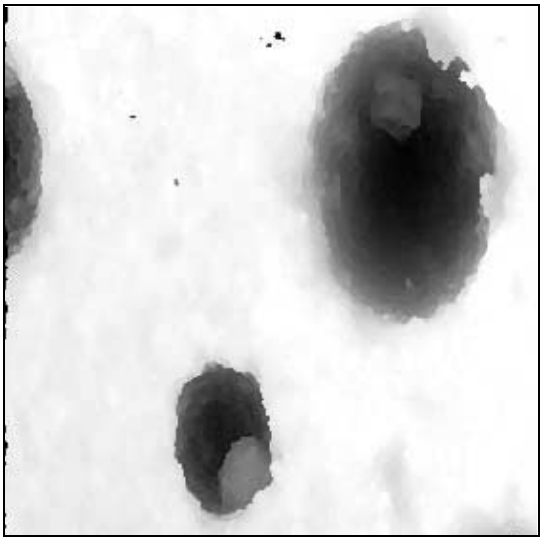

Fig. 6. Topographic image of a concrete sample.

and the bubbles boundaries. Some mathematical stereological tools allow an estimation of the three-dimensional size distribution based on a two-dimensional acquisition [3]. To perform the model with a good quality it is necessary to assume that the bubbles are spherical, which is nearly exact.

The use of a confocal acquisition is here very efficient. The sample appears as a small concrete block whose surface intersects a lot of air bubbles. As previously seen, the topographic image permits an estimation of the altitude corresponding to each pixel lying in the microscope field: in our case, the upper points are clear and those corresponding to the bubbles bottom are dark.

From this relief information, it is easy to derive an estimation of the radius and volume of each bubble (Fig. 7), according to the following formulae:

$$R^2 = r^2 + (R - (z_a - z_b))^2,$$

$$R = \frac{r^2}{2(z_a - z_b)} + \frac{(z_a - z_b)}{2},$$

$$V = \frac{4}{3}\pi R^3,$$

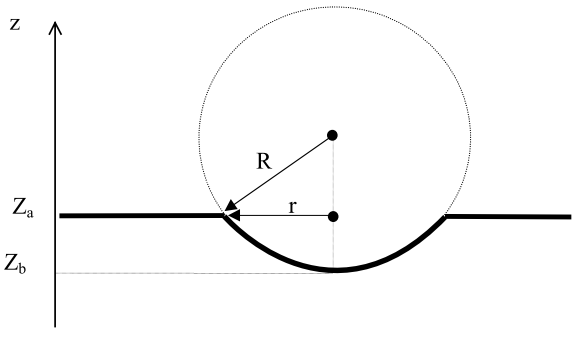

Fig. 7. Volume estimation of a bubble.

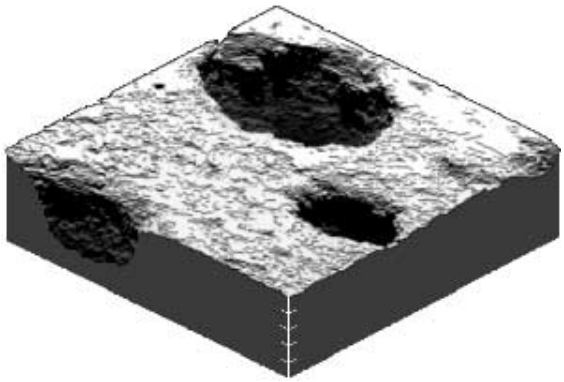

Fig. 8. A realistic view of the concrete surface.

where z_a corresponds to the average altitude of the concrete surface and z_b corresponds to the bubble bottom.

Finally, it is possible to merge the topographic image and the reflectance one, in order to obtain a realistic representation of the concrete surface (Fig. 8).

2.1. Some other applications

In order to prove the efficiency and the applicative area of confocal microscopy, let us look at some specific applications.

It is possible to observe a silicone replica of skin surface in order to estimate the size, depth and orientation of wrinkles (Fig. 9).

Various other applications are possible. In order to illustrate such a potential, we show an example concerning ceramics and another concerning an hair relief (Fig. 10).

From such illustrations, we note that the obtained images are not only esthetic ones but that they are extremely informative because of the quantified information they carry. A lot of other works dedicated to materials must be studied by the interested reader. Among them, we propose the Ph.D. thesis of S. Mathis [4].

2.2. Measurement precision

2.2.1. Theoretical spatial resolution

It is important to estimate the precision of a confocal 3D image. Here we refer to S. Martinez Ph.D. thesis [5], taking into account the formulae of Kino and Xiao [6]. The theoretical resolutions are given in Table 1.

2.2.2. Vertical precision

After noise filtering, we want to know the vertical precision in a topographic image. Early experiences [7] indicate an "a priori" value of 0.1–0.2 μm.

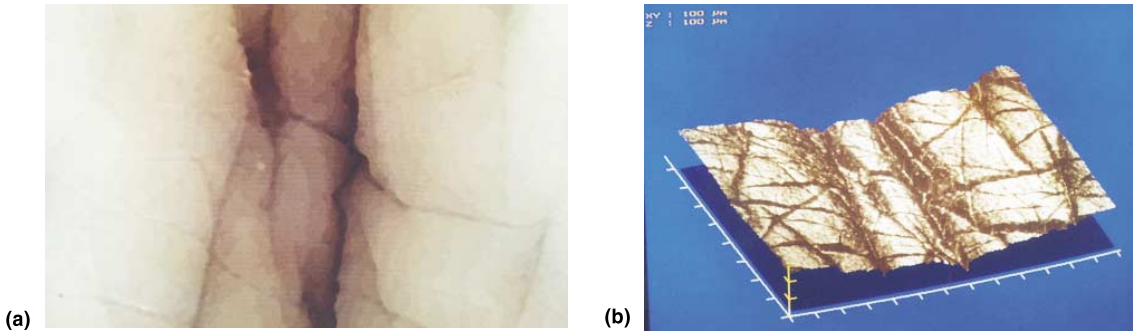

Fig. 9. Skin wrinkle: (a) Topographic image. (b) 3D realistic view.

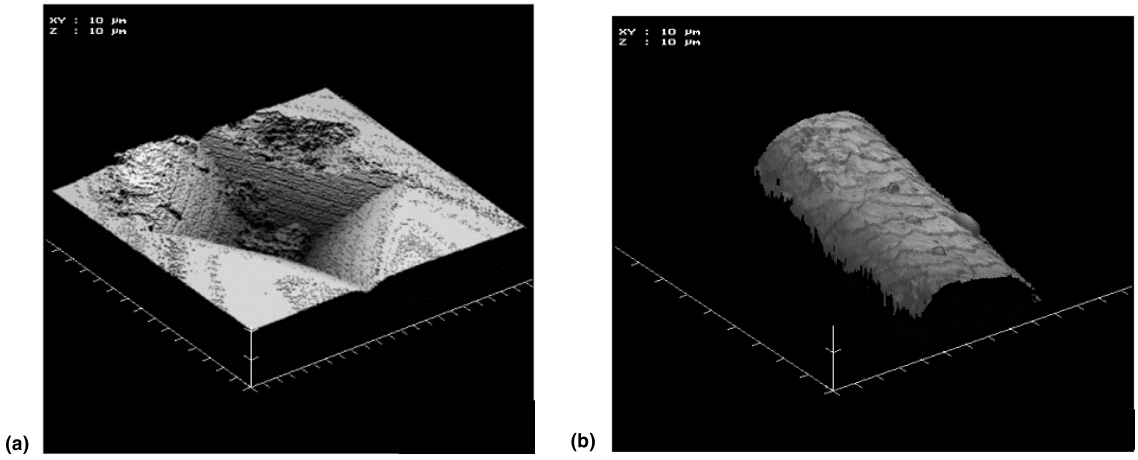

Fig. 10. (a) Ceramics stamping. (b) An hair scales.

Table 1
Theoretical spatial resolution of a confocal image

Resolution	Magnification/numerical aperture	Objective alone (μm)	Objective + Nipkow disk (μm)
Axial	×50/0.85	0.67	1.90
	×100/1.25	0.26	0.43
Lateral	×50/0.85	0.22	0.33
	×100/1.25	0.15	0.22

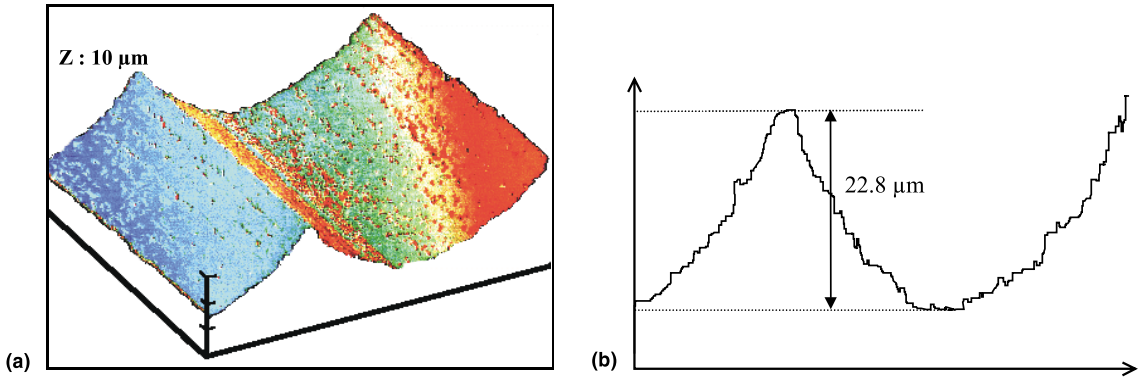

Fig. 11. (a) Used sample. (b) Depth measurement.

To confirm such values, dependent of the optical elements (objective...) and also of the mechanical structures of the TSM stage the same sample has been acquired under different magnifications, with a fixed resolution of 0.2 μm between each focusing plane.

For various objectives (×10, ×20, ×40, ×60, ×100) and for a fixed resolution of 0.2 μm, the measured depth of the sample is always of 22.80 μm (Fig. 11).

Thus the vertical resolution between two optical cuts is 0.2 μm.

3. Conclusion

The confocal approach is at the same time efficient, quantitative, and very precise (at the scale of a micrometer) and appears as a powerful and promising substitute to the more classical MEB images for material estimation.

References

[1] Wilson T. Confocal microscopy. London: Academic Press; 1990.
[2] Petran M, Hadravsky M, Egger D, Galambos R. J Opt Soc Am 1968;58:661–4.
[3] Gundersen HJG, Jensen EB. J Microsc 1987:147.
[4] Mathis S. Acquisition et analyse quantitative des images de micro reliefs en microscopie confocale et en microscopie à balayage électronique. Thèse de doctorat de l'Université de Caen, 1996.
[5] Martinez S. Contribution à la caractérisation des surfaces acquises en microscopie tridimensionnelle. Thèse de Doctorat de l'Université Jean Monnet de Saint-Etienne, 1998.
[6] Kino GS, Xiao GQ. Real-time scanning optical microscopes. In: Wilson T, editor. Confocal microscopy. London: Academic Press; 1990.
[7] Pawley B. Handbook of biological confocal microscopy. In: Pawley B, . New York: Plenum Press; 1990.